

Research Article

Achchhe Lal* and Kanif Markad

Nonlinear flexural analysis of sandwich beam with multi walled carbon nanotube reinforced composite sheet under thermo-mechanical loading

<https://doi.org/10.1515/cls-2020-0001>

Received Nov 05, 2019; accepted Mar 12, 2020

Abstract: Nonlinear flexural analysis of sandwich composite beam with multiwall carbon nanotube (MWCNT) reinforced composite face sheet and bottom sheet under the thermo-mechanically induced loading using finite element method is carried out. Solution of current bending analysis is performed using Newton's Raphson approach by using higher order shear deformation theory (HSDT) and non-linearity with Von Kármán kinematics. The sandwich laminated composite beam is subjected to uniform, linear and nonlinear varying temperature distribution through thickness of the beam. The sandwich beam with MWCNT reinforced composite facesheet and bottom sheet is subjected to point, uniformly distributed (UDL), hydrostatic and sinusoidal loading. The two phase matrix is utilized with E-Glass fiber to form three phase composite face sheet and bottom sheet by Halpin-Tsai model. The static bending analysis is performed for evaluating the transverse central deflection of three and five layered sandwich composite beam. Transverse central deflection is measured by varying CNT volume fraction, uniformly distributed, linearly and nonlinear varying temperature distribution, thickness ratio, boundary condition, number of walls of carbon nanotube by using interactive MATLAB code.

Keywords: flexural, FEM, HSDT, transverse central deflection, MWCNT

Nomenclature and Abbreviation

α_m	Thermal expansion coefficient of matrix
G_f	Shear modulus of conventional composite
E_f, ν_f	Longitudinal and poisson's ratio of conventional fiber
E_m, ν_m	Matrix material Young's modulus and poisson's ratio
$E_{cnt}, \nu_{cnt}, V_{cnt}$	Young's modulus, poisson's ratio and volume fraction of SWCNT/MWCNT
a, b, h	Length of beam, width of beam and thickness of beam
$ESMWCNTRSCB$	Elastically supported multiwall carbon reinforced sandwich composite beam
h, h_f, h_c	Sandwich composite total thickness, thickness of facesheet and thickness of core
l, d, h_{in}, t_{cnt}	Length, diameter, inner wall spacing and thickness of SWCNT
q, Q	Dimensional load and non-dimensional load parameter
$SWCNTR, MWCNTR$	Single Wall and Multi walled Carbon Nanotube Reinforced
T_1, T_2, T_0	Applied bottom temperature, top temperature through thickness of beam and room temperature
TCD	Transverse central deflection
W, W_0	Dimensional and dimensionless transverse central deflection

*Corresponding Author: Achchhe Lal: Mechanical Engineering Department, SVNIT, Surat, Gujarat, India. (395007); Email: achchhe.lal@med.svnit.ac.in; lalachchhe@yahoo.co.in; Tel.: +919824442503
 Kanif Markad: Research Scholar, Department of Mechanical of Engineering, SVNIT, Surat 395007, India; Email: kmarkad13@gmail.com



V. D. Patil
 PRINCIPAL
 Dr. Vithalrao Vikhe Patil
 College of Engineering
 Ahmednagar

1 Introduction

Instead of metallic counterparts, laminated composites are intensively used in various commercial and household applications because of superior mechanical and thermal properties. Furthermore, sandwich composite material is a special class of a composite which can utilize the combination of various materials that are bonded together to improve and utilize effectively the properties of each component to obtain the structural advantage of the overall assembly for optimum performance. The faces or skin are rigidly bonded to the core material to get a load transfer between the components. Against the wrinkling and buckling, the core is the one who resists the shear and settles it down.

Though laminated composite material having excellent longitudinal property, in case of sudden thermo-mechanical loading in the form of mechanical and /or thermal it is necessary to sustain it by the structural element. With little additional weight of core between the face and bottom sheet, stiffness and strength of the structure can be improved. In this paper, the various location of an isotropic core with laminated composite CNT reinforced face sheet and the bottom sheet has been utilized to increase the transverse central deflection. In sandwich composite material, the core is responsible to distribute the load and hence shear stresses over a wide area, and this causes the resistance against shear and compressive forces better than the use of only laminated composite material.

Here, the face sheet and bottom sheet are proposed to made of carbon nanotube reinforced laminated composite material. There are various approaches to find out the material property of the three-phase composite material property. the bending analysis over the single-wall carbon nanotube (SWCNT) reinforced in a functionally graded composite plate performed by Shen [1]. By the rule of mixture, the overall material property of the composite plate has been found out. Also, Fidelus *et al.* [2], Anumandla *et al.* [3], Shen and Xiang [4] utilized the rule of mixture and extended rule of mixture to find the effective elastic property of the composite structure. [4–11] utilized the Halpin-Tsai approach for the effective elastic properties of the composite material which they used. The explicit formulation for the Mori-Tanaka tensor which was utilized for the unidirectional (UD) FRC in Liu and Huang [12]. Effective material properties of the composite material are obtained by this Mori-Tanaka formulation.

Alebrahim *et al.* [13] reviewed the responses of the composite structure against the quasi-static loads. Charpy

and Izod pendulums, the falling weight fixtures experimental methods performed for demonstrating the response material. A two-layer fiber-reinforced composite sheet with a truss core under the application of compressive and impact loading and studied the mechanical responses by Xiong *et al.* [14]. The damage mechanism under the action of low-velocity impact was presented. Wang and co-author [15, 16] observed that impact loading plays a major problem during the design of laminated composite structure because structure with such kind of loading reduces stiffness and strength drastically which may not possible to see over the surface. They also investigated the residual strength and characteristics of the composite sandwich core. Observation shows that the study and design of laminated composite material create the major issues because of sudden impact which results in weakening strength and stiffness considerably which may not possible to see by necked eye.

A few papers were studied the static analysis of sandwich composite plates and beams. In the case of sandwich beams and plates, loading plays an important role as it directly affects performance/operation. The number of papers was studied the uniformly distributed, sinusoidal and point load, but very few articles were performed load-deflection analysis with all types of load. Mantari *et al.* [17] considered the cross-ply laminated composite plate with different lamination scheme and simple three-layered sandwich plate consist of one layer of core and other two of skins. For the analysis of the considered plate, a new trigonometric theory of shear deformation utilized. Maximum central plane deflection for the laminated composite plate and uniformly distributed force (UDL) were considered for a composite sandwich where stress variation found out. Also, Sahoo and Singh [18] considered laminated composite plate and sandwich plate with Single layer skin 0° for the analysis. The sandwich plate was examined with shear deformation theory for the transverse sinusoidal load. The vibrational analysis of a sandwich plate with piecewise shear deformation theory with the consideration of single layer orthotropic material in a sheet, performed by Zhao *et al.* [19]. The author was considered the examples based on vibrational analysis for the demonstration of effectiveness and exactness of the utilized theory. Mantari *et al.* [20] used layer wise displacement HSDT for bending analysis of sandwich composite plate as this new theory not depends upon layers and also accounting the non-linear and constant variation of in-plane and displacement through plate thickness.

Temperature also plays a vital role in the laminated and sandwich composite analysis because it directly affects the strength and stiffness of the beam. In the present

paper, the various temperature on distributions is considered to analyses the sandwich beam deflection analysis. Vidal *et al.* [21] studied the three-layered sandwich composite beam with variable separation and finite element discretization. The effect of sinusoidal temperature distribution was observed through-thickness of the sandwich composite. Li *et al.* [22] investigated the effect of the thermomechanical coupling over the sandwich panel with aluminum foam core closed cell. Effect of thermal conductivity, specific heat, and thermal-protective layer thickness studied over the sandwich panel. Thermomechanical response over the circular sandwich plate made from foam core and glass epoxy sandwich skins in Santiuste *et al.* [23]. Through the finite element and analytical models, thermal degradation of the core material of a circular sandwich plate has been studied by higher-order sandwich panel theory. Lal and Markad [24] performed the bending analysis over the CNT reinforced laminated composite beam based on HSDT and Von Kármán nonlinear analysis. The effect of temperature and mechanical loading over central deflection of the composite beam were observed with the variation of various parameters and observed the efficiency of the studied model over the conventional composite model. Karamanli [25] presented the bending behavior of sandwich and laminated composite beams with different boundary conditions by Ritz method and Timoshenko beam theory (TBT) and axial stress, shear stress, and deflection at middle span are calculated. Here, it is observed that fiber angle has a major effect on axial stress, shear stress and mid deflection of a beam for composite beams with different boundary conditions. Development in trigonometric shear deformation theory (TSDT) to understand the flexural behavior of sandwich beams where transverse displacement is the function of the longitudinal direction and axial displacement is expressed with trigonometric function by Ghugal and Shikhare [26]. The present theory is very efficient for the prediction of bending behavior and this theory does not require any shear correction factor. Gibson [27] presented a simplified material equation for the prediction of the flexural behavior of composite sandwich beams with loading in four-point bending. Result of the present model is compared with experimental and finite element analysis (FEA), where it is observed that this simplified model shows good result for CF/RC beam and sensibly well for the GF/RC beam. Yoon *et al.* [28] shown the instigation of nonlinear flexure behavior in deflection of sandwich beam with thermoplastic foam core for various face thickness by four-point bending. In this study analytical model with the incremental formulation is presented for the prediction of the nonlinear deflection of sandwich beam with foam core. Here, it

is confirmed that nonlinear stress-strain relation of sandwich beam with foam core essentially measured for the prediction of nonlinear deflection behavior. Thorat *et al.* [29] proposed the refined beam theory (RBT) for the bending analysis of soft-core sandwich beam where traction force-free conditions are implemented on top and bottom of the beam without using shear correction factor. The present result shows good agreements with the results from the exact solution and HSDT. Further, Sayyad and Ghugal [30] presented the applications of trigonometric shear deformation theory for the static flexural analysis of sandwich beam with softcore. The present theory is displacement-based and satisfies the condition of zero-stress over top and bottom surface without shear correction factor. Li *et al.* [31] studied the bending analysis of a sandwich plate with an orthotropic face sheet and functionally graded material (FGM) core by using double trigonometric series, here the core of plate is graded by a power-law distribution. According to literature, Young's modulus ratio of the top and bottom of the core has a major effect on the deflection of the plate. Effective utilization of Halpin-Tsai approach for the material property evaluation of composite material with CNT reinforcement done in Bhardwaj *et al.* [32]. It also presented a nonlinear flexural response using Chebyshev polynomials. Kumar and Srinivas [33] used the extended rule of mixture for the evaluation of effective material property of CNT reinforced composite material and perform the bending, buckling and vibration analysis. Deng and Lee [34] presented the carbon fiber reinforced polymer metallic beam static analysis. Also, different cases were studied for experimentation and shows different factors influencing metallic beam strength. Rouhi and Alavi [35] used the functionally graded SWCNT composite plate whose material properties were investigated by molecular dynamics simulations. The nonlinear composite plate analysis was carried out under the action of uniformly distributed load assuming temperature-dependent material properties. Singh *et al.* [36] performed the bending stochastic nonlinear analysis of laminated composite plate which is resting on a Pasternak elastic foundation. Mean and standard deviation of nonlinear TCD of the composite plate was obtained. Shen *et al.* [37] presented the bending, buckling and post buckling analysis of the graphene reinforced composite beam. Uniformly distributed and FG CNTRC beam considered for the study, and using micromechanical model material properties are found out. Along with these, Ferreira [38] provided the MATLAB simulation procedure for the laminated composite structures and sandwich structures for the two phase materials. Donthireddy and Chandrashekhara [39] presented a nonlinear dynamic and static response of the laminated composite beam un-

der the Thermomechanical load. Ply orientation of the laminated composite beam for different boundary conditions taken for the study. Kim and Lee [40] showed the response of functionally graded sandwich composite beam with the consideration of geometrical nonlinearity by Von Kármán sense. Numerical results were investigated for span-to-height ratio, boundary condition, gradient index, a material ratio over the FG sandwich beam. Finally, Gdoutos and Zacharopoulos [41] considered the foam sandwich beam for the load-deflection analysis under a three-point bending load. Also, for experimental analysis, nonlinear mechanics of material were considered.

From the available literature, it is observed that researchers tried to increase the strength and stiffness of composite structure with sandwiching the core material between the skins by the application of various loading for optimum performance. Relatively very little work available related to bending analysis over the sandwich composite with face sheet and bottom sheet is of carbon nanotube-reinforced composite with various lamination scheme without considering the effect of linear, nonlinear and uniformly distributed temperature distribution. Also, no literature gave attention to the evaluation of the effect of various lamination scheme with variation in the laminate and core thickness and their places along with various temperature distribution, and effect of different forces over the laminated sandwich composite beam, as per author's knowledge. Also in this study of sandwich composite beam consist of SWCNT and MWCNT reinforced face sheet and bottom sheet, implementing two-phase matrix with fiber have been considered.

So for the present study SWCNT/MWCNT reinforced sandwich composite beam is utilized for the bending analysis under the thermo-mechanical effect. This paper will emphasize some of the most significant progress in the design of sandwich composite structures and in the analysis of their response to uniformly distributed, hydrostatic, point and sinusoidal loading under different temperature distribution.

2 General formulation

2.1 Geometrical configuration of the sandwich composite beam

Figure 1 shows the laminated composite sandwich beam of length a , width b , thickness h and material direction of the typical lamina is (x, z) coordinate system. It consists of face sheet and bottom made of MWCNT reinforced with glass

fiber and core is at the center of the beam. Facesheet and bottom sheet are made of a two-layered laminated composite which may have a different orientation. The individual thickness of the laminated composite beam is denoted by h_f , the thickness of core defined by h_c and overall thickness of the sandwich beam is h , as shown in the figure. It is assumed that a perfect bonding exists between cores and face sheets and bottom sheet so that no slippage can occur at the interface.

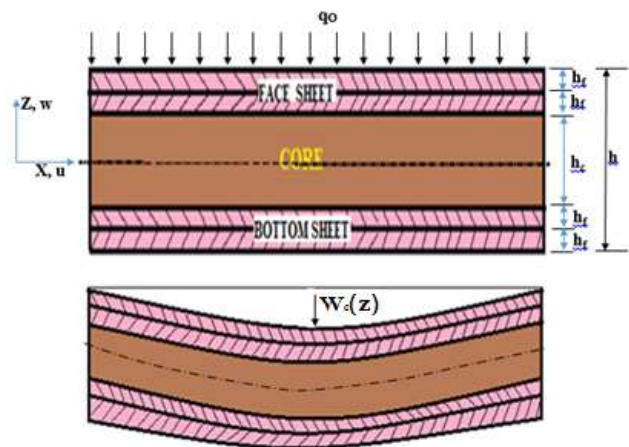


Figure 1

Uniformly distributed load is applied over facesheet of sandwich beam shown by q_0 and W_0 is the transverse central deflection occurred in sandwich beam along z direction. In present analysis along with uniformly distributed load, hydrostatic, point and sinusoidal loading is applied over the face sheet of sandwich composite beam. Figure 2 shows the nature of these different loading.

2.2 Material properties of carbon nanotube reinforced composite by Halpin-Tsai model

The effective elastic property of three phase composite material are evaluated using Halpin-Tsai approach. MWCNT added in epoxy to formulate new kind of two phase matrix reinforced in fiber and form three phase laminated composite material which is further utilized in face sheet and bottom sheet, to improve overall material property for the facesheet and bottom sheet of sandwich composite beam shown in Figure 1. Two phase matrix property evaluated as, [24, 32].

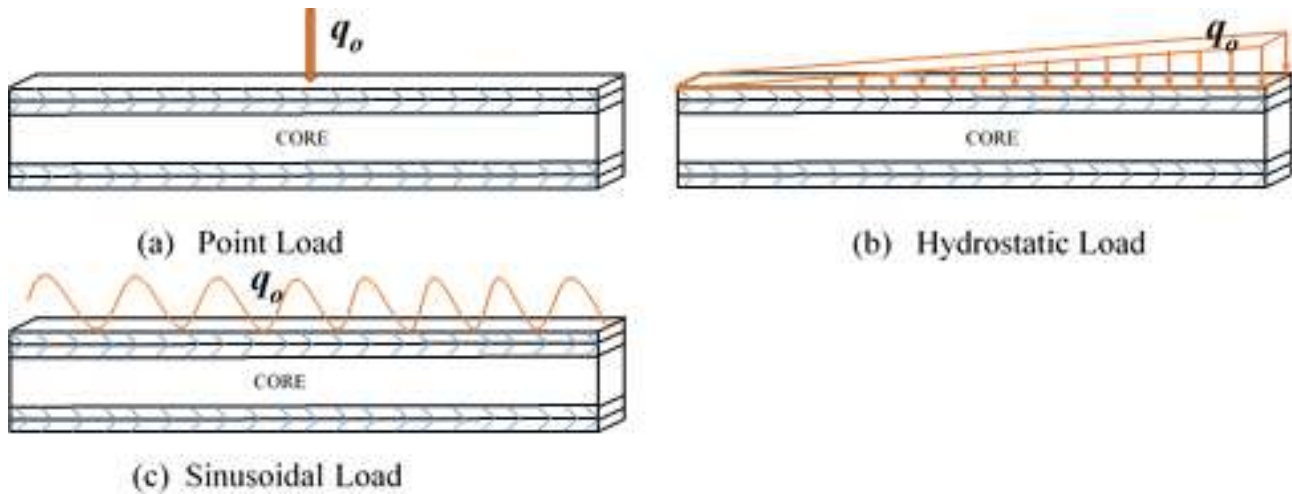


Figure 2

$$E_M = \left\{ \left(\frac{3}{8} \right) \left[\frac{1 + \xi_L \frac{(E_{CNT}/E_m)-1}{(E_{CNT}/E_m)+2(L/t)} V_{CNT}}{1 - \frac{(E_{CNT}/E_m)-1}{(E_{CNT}/E_m)+2(L/t)} V_{CNT}} \right] + \left(\frac{5}{8} \right) \left[\frac{1 + \xi_T \frac{(E_{CNT}/E_m)-1}{(E_{CNT}/E_m)+2(L/t)} V_{CNT}}{1 - \frac{(E_{CNT}/E_m)-1}{(E_{CNT}/E_m)+2(L/t)} V_{CNT}} \right] \right\} \quad (1)$$

Where, Young's modulus of epoxy, length and thickness of CNT defined by E_m , L , t . CNT thickness can be calculated as, [33]

$$t = \frac{1}{2} \left[\frac{\sqrt{3(m^2 + n^2 + mn)}}{\pi} a_{c-c} + t_{cnt} + 2(N_w - 1)h_{in} - \frac{\sqrt{3(m^2 + n^2 + mn)}}{\pi} a_{c-c} - t_{cnt} \right] \quad (2)$$

Where (m, n) defines chirality of carbon nanotube, a_{c-c} carbon-carbon bond length of single walled CNT, $a_{c-c} = 0.335$ nm. $h_{in} = 1.5t_{cnt}$. Two phase matrix (E_M) is reinforced along with the E-Glass fiber orthotropically. Now the longitudinal modulus of the three phase composite evaluated as, [30, 32]

$$E_1 = E_f V_f + E_m V_m \quad (3)$$

The transverse and in-plane shear modulus of composite are expressed as,

$$E_2 = \left[\frac{1 + \xi_T \frac{(E_f/E_m)-1}{(E_f/E_m)+2} V_{CNT}}{1 - \frac{(E_f/E_m)-1}{(E_f/E_m)+2} V_{CNT}} \right] E_m; \quad (4)$$

$$G_{12} = \left[\frac{1 + \xi_T \frac{(G_f/G_m)-1}{(G_f/G_m)+1} V_{CNT}}{1 - \frac{(G_f/G_m)-1}{(G_f/G_m)+1} V_{CNT}} \right] G_m;$$

The Poisson's ratio of composite can be expressed as:

$$\nu_{12} = \nu_f V_f + \nu_m V_m \quad (5)$$

By the Shapery model, the effective coefficient of thermal expansion along longitudinal and transverse direction evaluated as, [1]

$$\alpha_{11} = \frac{V_{CNT} \alpha_{11}^{CNT} E_{11}^{CNT} + V_m E^M \alpha^m}{E_{11}^{CNT} V_{CNT} + V_m E^M}; \quad (6)$$

$$\alpha_{22} = \left(1 + \nu_{12}^{CNT} \right) \alpha_{22}^{CNT} V_{CNT} + V_m \alpha^m (1 + \nu^m) - \nu_{12} \alpha_{11}$$

Where, $\alpha^m = 45(1 + 0.0005\Delta T)10^{-6}$

It is assumed that matrix and CNT properties are the temperature functions, therefore effective material properties of CNTRCs are also the temperature (T) functions.

2.3 Displacement field model

For a CNT reinforced composite beam, the displacement field components shown as the modified components along x and z directions of an arbitrary point within the beam based on the HSDT using continuity C° so as to minimize difficulties in computational can be expressed as, [22, 33, 37, 38],

$$\bar{u}(x, z) = u + f_1(z)\psi_x + f_2(z)\phi_x; \quad \bar{w}(x, z) = w; \quad (7)$$

Where u , w are the mid-plane axial and transverse displacement, ψ_x is the rotation of normal to the mid-plane along y -axis and $\phi = \partial w / \partial x$ is the slope along x -axis, respectively. The parameter $f_1(z)$ and $f_2(z)$ are expressed as,

$$f_1(z) = C_1 z - C_2 z^3, \quad f_2(z) = -C_2 z^3, \quad (8)$$

with $C_1 = 1$, $C_2 = 4/3h^2$

For the lowest computational efforts without affecting the accuracy of solution, C° continuous isoparametric FEM with four degrees of freedom (DOFs) per node is proposed.

The displacement vector for the modified C° continuous model can be written as,

$$\{q\} = \begin{bmatrix} u & w & \phi_x & \psi_x \end{bmatrix}^T \quad (9)$$

2.4 Strain displacement relation

The total strain vector consisting of linear strain, non-linear strain (Von Kármán type), and thermal strains vectors associate with the displacement for MWCNRCB can be defined as

$$\{\bar{\epsilon}\} = \{\bar{\epsilon}^L\} + \{\bar{\epsilon}^{NL}\} - \{\bar{\epsilon}^T\} \quad (10)$$

Where thermal strain vector defined as, $\{\bar{\epsilon}^T\} = \{\alpha_1 \Delta T \quad \alpha_2 \Delta T \quad 0 \quad 0 \quad 0\}$

From Eq. (10), the linear and nonlinear strain tensor can be written as,

$$\bar{\epsilon}^L = [B]\{q\}; \text{ and } \bar{\epsilon}^{NL} = \frac{1}{2} [A_{nl}] \{\phi_{nl}\} \quad (11)$$

Where $[B]$ and $\{q\}$ are the geometrical matrix and displacement field vector and

$$\{A_{nl}\} = \frac{1}{2} \left[\frac{\partial w}{\partial x} \right]^T \text{ and } \{\phi_{nl}\} = \left\{ \frac{\partial w}{\partial x} \right\} \quad (12)$$

The thermal strain vector $\{\bar{\epsilon}^T\}$ induced by uniform, linear or nonlinear temperature change can be expressed as,

$$\{\bar{\epsilon}^T\} = \{\alpha_x\} \Delta T \quad (13)$$

Where $\{\alpha_x\}$ and ΔT are the thermal expansion coefficients in x direction, and the change in temperature in the MWCNTRCB respectively and can be expressed as [34], Uniform temperature distribution,

$$\Delta T = T_1 - T_0 \quad (14a)$$

Linearly varying temperature distribution,

$$\Delta T = \left(T_1 + \frac{z}{h} T_2 \right) - T_0 \quad (14b)$$

Nonlinearly varying temperature,

$$\Delta T = \left(T_1 + \frac{z^2}{h} T_2 \right) - T_0 \quad (14c)$$

Where T_1 is the bottom temperature and T_2 is the top temperature of sandwich beam respectively. The parameter T_0 is the ambient temperature taken as 300K.

2.5 Stress-strain relation

For the plane stress case, the stress-strain relationship can be written as, [34]

$$\{\bar{\sigma}\} = [Q] \{\bar{\epsilon} - \bar{\epsilon}^T\} \quad (15)$$

$$\begin{Bmatrix} \bar{\sigma}_x \\ \bar{\tau}_{xz} \end{Bmatrix} = \begin{bmatrix} \bar{Q}_{11} & 0 \\ 0 & \bar{Q}_{55} \end{bmatrix} \left\{ \{\bar{\epsilon}^L\} + \{\bar{\epsilon}^{NL}\} - \{\bar{\epsilon}^T\} \right\} \quad (16)$$

Where,

$$\begin{aligned} \bar{Q}_{11} &= Q_{11} \cos^4 \theta_k + Q_{22} \sin^4 \theta_k \\ &\quad + 2(Q_{12} + 2Q_{66}) \cos^2 \theta_k \sin^2 \theta_k, \\ \bar{Q}_{55} &= Q_{55} \cos^2 \theta_k + Q_{44} \sin^2 \theta_k \end{aligned} \quad (16a)$$

With

$$\begin{aligned} Q_{11} &= \frac{E_1}{1 - \nu_{12}\nu_{21}}; \quad Q_{22} = \frac{E_2}{1 - \nu_{12}\nu_{21}}; \\ Q_{12} &= \frac{\nu_{12}E_2}{1 - \nu_{12}\nu_{21}}; \quad \nu_{21} = \frac{\nu_{12}E_2}{E_1}; \\ Q_{55} &= G_{12}; \quad \text{and} \quad Q_{44} = G_{13} \end{aligned} \quad (17)$$

Here θ_k is represented as fiber orientation. The parameters E_1 , E_2 , G_{12} , G_{13} , G_{23} , and ν_{12} are the longitudinal, transverse and shear modulus, and Poisson's ratio, respectively.

2.6 Strain energy of MWCNTRC beam

The strain energy (Π_1) of the MWCNTRC beam which is under the large deformation can be expressed as,

$$\Pi_1 = U_L + U_{NL} \quad (18)$$

The linear strain energy (UL) of the MWCNTRC beam is written as

$$\begin{aligned} U_L &= \int_A \frac{1}{2} \{\bar{\epsilon}^L\}^T [Q] \{\bar{\epsilon}^L - \bar{\epsilon}^T\} dA \\ &= \int_A \frac{1}{2} \{\bar{\epsilon}^L\}^T [D - D_{th}] \{\bar{\epsilon}^L\} dA \end{aligned} \quad (19)$$

Where $[D]$, $[D_{th}]$, $\{\bar{\epsilon}^L\}$ and $\{\bar{\epsilon}^T\}$ are the elastic stiffness matrix and linear strain vector with thermal effect, respectively.

The nonlinear strain energy (U_{NL}) of the MWCNTRC beam can be rewritten as

$$\begin{aligned} U_{NL} &= \int_A \frac{1}{2} \{\bar{\epsilon}^L\}^T [D_1 - D_{1th}] \{\bar{\epsilon}^{NL}\} \\ &\quad + \frac{1}{2} \{\bar{\epsilon}^{NL}\}^T [D_2 - D_{2th}] \{\bar{\epsilon}^L\} \end{aligned} \quad (20)$$

$$+ \frac{1}{2} \left\{ \bar{\varepsilon}^{NL} \right\}^T [D_3 - D_{3th}] \left\{ \bar{\varepsilon}^{NL} \right\} dA$$

Where D_1 , D_2 , D_3 , D_{1th} , D_{2th} and D_{3th} are the elastic stiffness matrices of the MWCNTRC beam with thermal effect, respectively.

$$\begin{aligned} \text{Here, } [D_1] &= \begin{bmatrix} A_{11} & B_{11} & E_{11} \end{bmatrix}^T; [D_2] = [D_1]^T; [D_3] = \\ &[A_{11}] \text{ and } [D_{1th}] = \begin{bmatrix} A_{11th} & B_{11th} & E_{11th} \end{bmatrix}^T; [D_{2th}] = \\ &[D_{1th}]^T; [D_{3th}] = [A_{11th}]; (A_{11}, B_{11}, D_{11}, E_{11}, F_{11}, H_{11}) = \\ &\int_{-h/2}^{h/2} Q_{11} \left(1, z, z^2, z^3, z^4, z^6 \right) dz \left(A_{11th}, B_{11th}, D_{11th}, \right. \\ &E_{11th}, F_{11th}, H_{11th} \left. \right) = \int_{-h/2}^{h/2} Q_{11} \left(1, z, z^2, z^3, z^4, z^6 \right) \\ &\alpha \Delta T dz \end{aligned}$$

2.7 Work done due to external applied loading

Work done due external applied load can be written as

$$\Pi_2 = W_q = \int_A q_m(x, z) w dA \quad (21)$$

Here, $q_m(x, z)$ is the intensity of applied uniformly distributed load.

For the uniformly distributed loading $q_m(x, z)$ is written as

$$q_m(x, z) = \frac{QE_m I}{a^3} \quad (22a)$$

For the sinusoidal distributed loading $q_m(x, z)$ is written as

$$q_m(x, z) = \frac{QE_m I}{a^3} \sin\left(\frac{\pi x}{a}\right) \quad (22b)$$

For the hydrostatic distributed loading $q_m(x, z)$ is written as

$$q_m(x, z) = \frac{QE_m I}{a^3} \left(\frac{x}{a}\right) \quad (22c)$$

For the point loading $q_m(x, z)$ is written as

$$q_m(x, z) = \frac{QE_m I x}{a^3} \quad (22d)$$

Where, Q and I are the uniform distributed load parameters and Moment of inertia, respectively. x is the location of nodes where sinusoidal and point load applied.

2.8 Finite element formulation

In the present paper, a C^0 continuity for one-dimensional Hermitian beam element with 4 DOFs per node is employed. Displacement and field vector from Eq. (9) can be

written as, [2]

$$\{q\} = \sum_{i=1}^{NN} N_i \{q\}_i; \quad x = \sum_{i=1}^{NN} N_i x_i; \quad (23)$$

Where, N_i , $\{q\}_i$ NN, x_i = interpolation function for the i^{th} node, vector of unknown displacements for the i^{th} node, the number of nodes per element, Cartesian coordinate respectively.

The linear interpolation for axial displacement and rotation of normal and Hermite cubic interpolation functions are chosen for transverse displacement and slope. Using finite element model Eq. (23), Eq. (18) can be expressed as,

$$\prod_1 = \sum_{e=1}^{NE} \prod_a^{(e)} = \sum_{e=1}^{NE} \left(U_L^{(e)} + U_{NL}^{(e)} \right) \quad (24)$$

Where, NE and (e) denote the number of elements and elemental, respectively.

Eq. (24) can be further expressed as,

$$\begin{aligned} \Pi_1 &= \frac{1}{2} \sum_{e=1}^{NE} \left[\{q\}^{T(e)} \left([K_I + K_{nl}]^{(e)} \right. \right. \\ &\quad \left. \left. - [K_{lth} + K_{nlth}]^{(e)} \right) \{q\}^{(e)} \right] \\ &= \{q\}^T \left[(K_I + K_{nl}) - (K_{lth} + K_{nlth}) \right] \{q\} \end{aligned} \quad (25)$$

Here

$$[K_{nl}] = \frac{1}{2} [K_{nl1}] + \frac{1}{2} [K_{nl3}]$$

Where $[K_I]$, $[K_{lth}]$, $[K_{nl1}]$, $[K_{nl2}]$, $[K_{nl3}]$ and $\{q\}$ are defined as global linear, nonlinear stiffness matrices of plate and thermal effect and global displacement vector, respectively.

$$K_I^{(e)} = \frac{1}{2} \int_A [B]^{(e)T} D [B]^{(e)} dA;$$

$$K_{nl}^{(e)} = \frac{1}{2} \int_A [B]^{(e)T} D_1 [B]^{(e)} dA;$$

$$K_{nl1}^{(e)} = \frac{1}{2} \int_A [B]^{(e)T} D_2 [B]^{(e)} dA;$$

$$K_{nl2}^{(e)} = \frac{1}{2} \int_A [B]^{(e)T} D_3 [B]^{(e)} dA$$

$$K_{nlth}^{(e)} = \frac{1}{2} \int_A [B]^{(e)T} D_{1th} [B]^{(e)} dA;$$

$$K_{nlth1}^{(e)} = \frac{1}{2} \int_A [B]^{(e)T} D_{2th} [B]^{(e)} dA;$$

$$K_{nlth2}^{(e)} = \frac{1}{2} \int_A [B]^{(e)T} D_{3th} [B]^{(e)} dA$$

2.9 Governing equation of bending

Using the Variational principle, governing equation for the nonlinear static analysis can be derived, with generalize based on the principle of virtual displacement. For the flexural analysis, the minimization of first variation of total potential energy ($\Pi_1 - \Pi_2$) with respect to displacement vector is defined by,

$$\partial (\Pi_1 - \Pi_2) = 0 \quad (26)$$

By substituting the Eq. (18), Eq. (19), Eq. (20), Eq. (21) and Eq. (26) obtained as,

$$([K] - \lambda [K_g]) \{q\} = \{F\} \quad (27)$$

With, $[K] = [K_l + K_{nl}]$; $[K_g] = [K_{lth} + K_{nlth}]$ and $\lambda = \alpha_{11} \Delta T \left(\frac{a}{h}\right)^2 (T_1 + T_2)$;

The stiffness matrix $[K]$ consists of linear and nonlinear plate and foundation stiffness matrices and geometric stiffness matrix $[K_g]$. The parameters $\{q\}$ and $\{F\}$ are the transverse deflection and force vector respectively.

The solution of Eq. (27) can be obtained using standard solution procedure such as direct iterative, incremental and/ or Newton-Raphson method etc. However, Newton Raphson method is one of the most popular and widely used solution procedure due to fast convergence at higher amplitude.

2.10 Solution approach: Newton Raphson method

The system of nonlinear static Eq. (27), can be written as [28],

$$[K(\{q\})] \{q\} = \{F\} \quad (28)$$

Here $[K(\{q\})]$ is the global nonlinear stiffness matrix, which is function of unknown global nodal displacement vector $\{q\}$ and global force vector $\{F\}$

1. The nonlinear matrix is assume as zero and evaluate the nodal displacement $\{q\}$ by taking linear stiffness matrix.
2. The nodal force vector $\{F\}$ is normalized.
3. For the defined maximum force at the plate center, the force vector $\{F\}$ is scaled up by C times so that resultant $\{F\}$ will have a force C at the maximum nodal force.
4. Utilizing scaled up force (normalized), the nonlinear stiffness matrix is obtained. The problem may now again have treated as static equation with new updated stiffness matrix.
5. Steps 2 to 4 are repeated by replacing by replacing $\{q\}$ linear to nonlinear $\{q_{nl}\}$ in steps (1) and (2), to

obtained converged displacement with prescribed accuracy of 10^{-3} . The detail solution procedure to find the transverse central deflection of MWCNTR sandwich beam is shown in Figure 3.

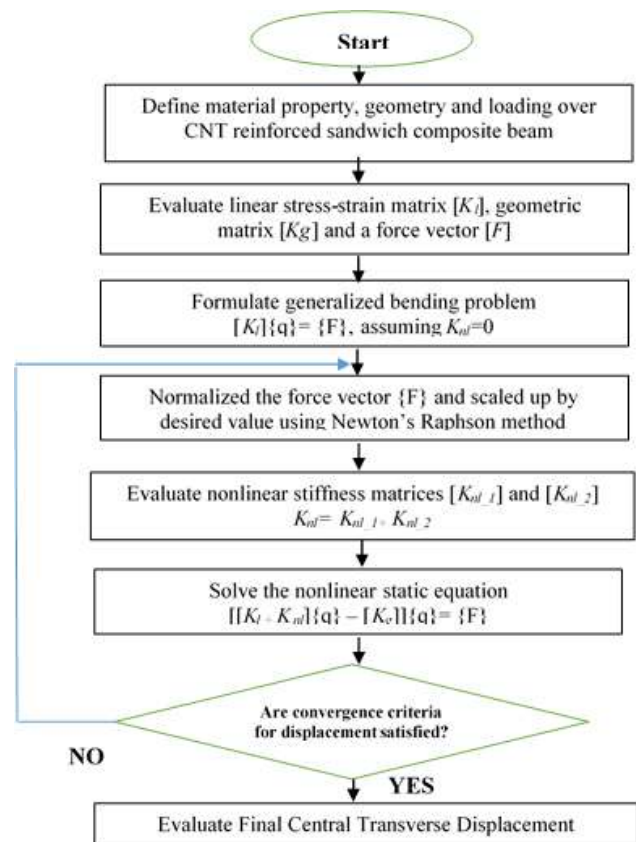


Figure 3

3 Results and discussion

In the present study, the nonlinear static transverse central deflection (TCD) response of multiwall carbon nanotube reinforced sandwich composite beam (MWCNTRSCB) subjected to uniformly distributed, sinusoidal, hydrostatic and point load is examined. Newton Raphson technique is proposed here to solve the nonlinear governing equation of beam. A user interactive computer program in MATLAB [R2015a] environment has been developed to evaluate the numerical results. Two node beam element with four DOFs per element is used for the present analysis.

The various boundary conditions are used as, Edges/ends are simply supported (SS): $u = w = 0$; at $x = 0, a$

Table 1: Effect of SWCNT volume fraction on mechanical property of SWCNTR sandwich composite beam

V_{cnt}	$E_1(10^{10})$ Pa	$E_2(10^{10})$ Pa	$G_{12}(10^9)$ Pa	ν_{12}	ν_{21}	$\alpha_1(10^{-6})/^{\circ}\text{C}$	$\alpha_2(10^{-6})/^{\circ}\text{C}$
0.05	1.3834	1.2013	4.5277	0.296	0.2570	20.41	49.86
0.10	2.4793	2.2702	8.57844	0.292	0.2674	13.693	49.323
0.15	3.5341	3.3700	1.28624	0.288	0.2746	10.557	47.692
0.20	4.5438	4.44625	1.71562	0.284	0.2779	8.7404	45.66
0.25	5.5042	5.46469	2.12778	0.280	0.2779	7.555	43.44
0.30	6.4095	6.40414	2.50933	0.276	0.2758	6.721	41.11
0.35	7.25449	7.25141	2.85109	0.272	0.2719	6.103	38.72
0.40	8.03218	7.99831	3.14760	0.268	0.2668	5.625	36.28

Edges/ends are clamped (CC): $u = w = \theta x = \psi x = 0$; at $x = 0, a$

One end is clamped and other edge is simply supported (CS): $u = w = \theta x = \psi x = 0$; at $x = 0$ and $u = w = 0$; at $x = a$

One end is free and other is clamped (FC): $u = w = \theta x = \psi x = 0$; at $x = a$

One end is free and other is simply supported (FS): $u = w = 0$; at $x = a$

The detailed numerical solution for the flexural analysis of sandwich composite beam subjected to static loading with thermal environment for sandwich composite composed of single walled carbon nanotube reinforced composite (SWCNTRC) and multi walled CNTRC face sheet and bottom sheet with isotropic middle core is presented. The effective material properties of MWCNTRCs is determined by using Halpin-TSai approach. Poly-methyl methacrylate (PMMA), is selected as a matrix, and its material properties assumed as $E_m = 2.5$ GPa $\nu_m = 0.3$, $\rho_m = 1180$ Kg/m³. The (10, 10) arm chair SWCNT is reinforced into the matrix to get the new two phase matrix, for that material properties are selected as, $E_{cnt} = 1.0$ TPa, $\rho_{cnt} = 1300$ Kg/m³, $\nu_{cnt} = 0.28$, $L_{cnt}/d_{cnt} = 100$, $h_{in} = 1.5 \times t_{cnt}$ and $\alpha_{11} = 5.168 \times 10^{-6}$ also in the present study it is assumed that α_{11} is constant for all layers including core.

The material properties the E-glass fiber are taken as in the form of Young's modulus, shear modulus and Poisson's ratio as $E_f = 69$ GPa, $G_f = 28.28$ GPa and $\nu_f = 0.22$ respectively.

Here analysis is performed over laminated three and five layered sandwich composite beam, for that core properties selected as, [38]

$$Q_C = \begin{bmatrix} 0.999781 & 0.231192 & 0 & 0 & 0 \\ 0.231192 & 0.999781 & 0 & 0 & 0 \\ 0 & 0 & 0.262931 & 0 & 0 \\ 0 & 0 & 0 & 0.266810 & 0 \\ 0 & 0 & 0 & 0 & 0.159914 \end{bmatrix}$$

Table 1 shows the variation of elastic moduli of SWCNT reinforced three phase composite material property with CNT volume fraction. As the volume fraction of carbon nanotube increases into the two phase matrix material, the overall elastic moduli also increases.

3.1 Convergence and validation study

Figure 4 illustrates the convergence study using FEM for the transverse central deflection of beam with variation in the number of elements and under boundary condition of CC, SS support. From the 16 number of elements, graph starts to converge, so from the study, 30 number of elements were selected for the further study. As the number of elements were increases, it is ensured to have monotonic convergence of solution, when utilized the complete and compatible displacement function.

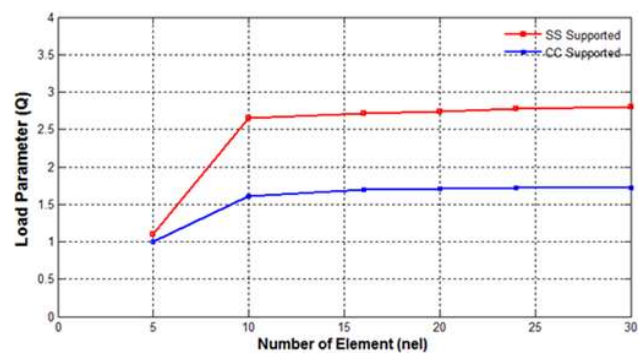
**Figure 4**

Figure 5 shows the validation study for the SWCNTRC beam with FG-CNTRC beam under uniformly distributed SWCNT beam. There is close agreement observe between present result and in Shen *et al.* [1] using semi analytical method.

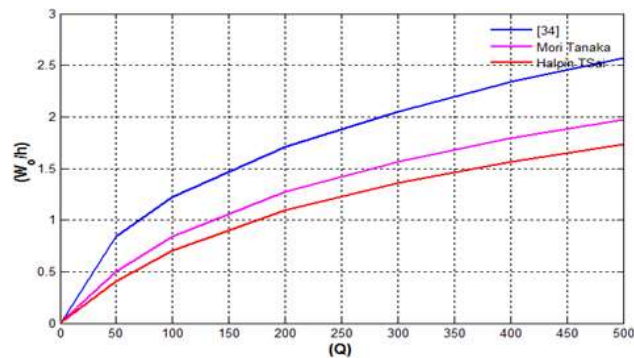


Figure 5

3.2 Parametric study

Figure 6 elaborate the effect of different support conditions on dimensionless maximum central transverse deflection of sandwich composite beam with variation in load parameter. The sandwich beam considered of three layered, made of laminated composite facesheet and bottom sheet, $[90/C/90]$, $a/h=10$. It is concluded that, among the clamp-clamp supported (CC), clamped-free supported (CF), clamped-simply supported (CS), hinged-simply supported (HS) and simply supported (SS) boundary condition, minimum transverse central deflection for laminated sandwich composite beam is observed at CC supported condition due to more number of constraints in provided boundary condition. As compared to CF, about 50% less deflection is observed in case of CC support condition.

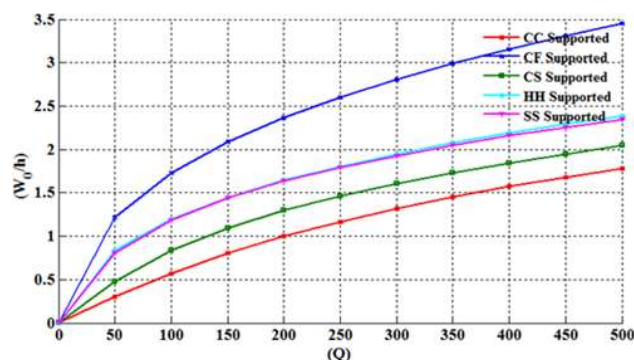


Figure 6

Figure 7 shows the nature of load deflection curve for linear and nonlinear analysis of $[90/C/90]$ sandwich beam. It is observed that transverse central deflection (TCD) follows linear nature during linear analysis and nonlinear nature in nonlinear analysis and there is always minimum deflection observe in presence of nonlinearity.

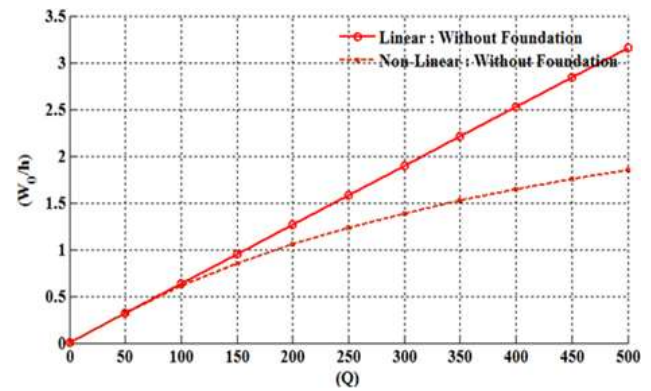


Figure 7

Figure 8 shows the variation in TCD with the variation in load parameter and SWCNT volume fraction in three and five layered sandwich composite beam made of facesheet and bottom sheet is of single walled carbon nanotube reinforced composite beam. Lamination scheme for five layered sandwich is $[90/30/C/30/90]$ and for three layered sandwich is $[0/C/0]$. During the analysis temperature is maintained at 300K, under the C-C boundary condition. As the CNT volume fraction increases in the sandwich composite beam, the TCD decreases in the proportion. From the figure, it is observed that, for 0.1% CNT volume fraction, there is approximately 51-52% decrease in deflection, for 0.2% CNT volume fraction, there is approximately 47-48% decrease in deflection, for 0.3% CNT volume fraction, there is approximately 46-47% decrease in deflection and for 0.4% CNT volume fraction, there is approximately 45-46% decrease in deflection.

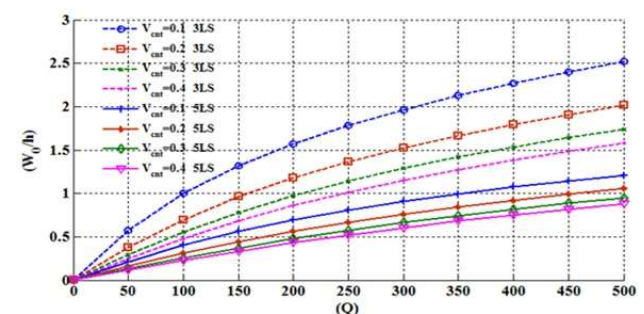


Figure 8

Figure 9 demonstrate the effect of variation in beam thickness ratio of the sandwich beam over TCD with load parameter. It is observed that as (a/h) increases, the transvers deflection of the beam also increases and this is due to decrease in the transverse resistant with respect to beam thickness.

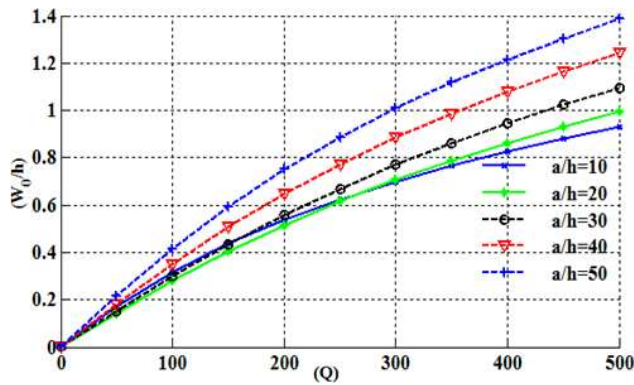


Figure 9

Figure 10 shows the (a) effect of variation in volume fraction of CNT on the transverse deflection of the SWCNTR five layered sandwich composite beam with [90/30/C/30/90] under the CC boundary condition for $a/h=20$. As the volume fraction of CNT increases, the transversal deflection in the beam reduced down and maximum transverse deflection is observed at the center of the beam. When CNT variation vary from 0.1 to 0.2, then about 25% reduction in deflection observe, and average reduction in deflection is approximately 16-17% takes place because of variation in stiffness of beam. Depending upon requirement one can utilize the fraction of CNT in sandwich composite. While (b) shows the comparison between FG-CNT reinforced beam with SWCNTRCB [90/30/0/30/90] and five layered SWCNTRSCB for the volume fraction of 0.12. It is concluded from the figure that, there is a minimum TCD observed in sandwich beam at the center, and also graph follow the same nature for all beam.

Figure 11 shows the effect of various loads on transverse central deflection over the three layered sandwich laminated composite beam and SWCNTR laminated composite beam under variation in load parameters, $V_{cnt}=0.2$, $a/h=0.15$, CC boundary conditions, [90/C/90], [90/0/90]. Observation shows that, there is a minimum TCD produced in sandwich composite beam as compared to SWCNTR laminated composite beam, also the point loading shows the highest deflection as compared to UDL, sinusoidal and hydrostatic loading. So there is much precaution is necessary during design of sandwich beam under point load. Also TCD produced in case of UDL is 5-7% and about 50% more as compared to sinusoidal and hydrostatic load respectively for the sandwich and laminated composite beam.

Figure 12 shows the effect of variation in normal and shear stresses of the SWCNTR three layered laminated composite beam with thickness direction (z/h) along longitudinal and transverse directions with [0/90/0] under the

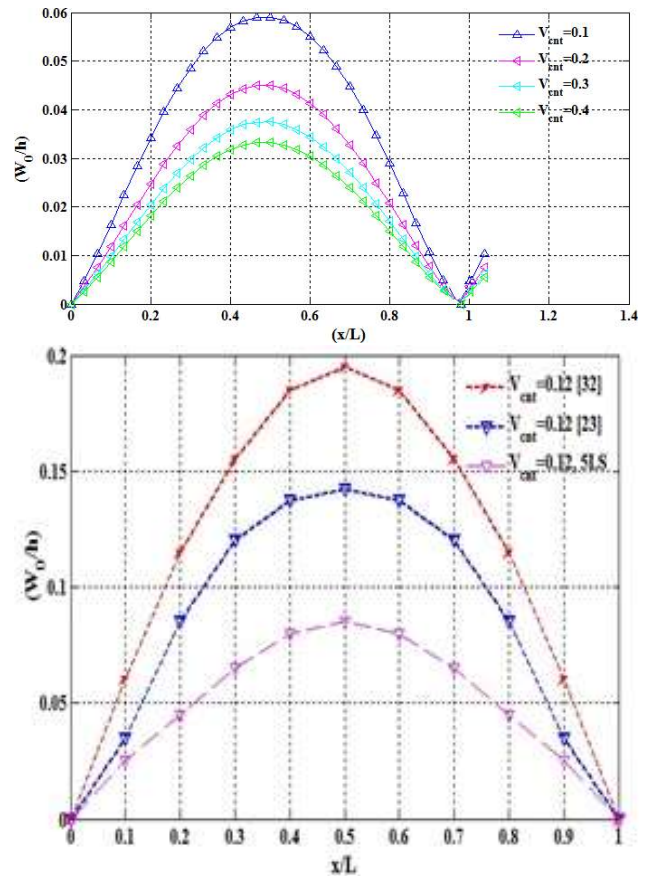


Figure 10

UDL and CC boundary condition. The effect of longitudinal stress is higher as compared to transverse stress.

Figure 13 shows the effect of variation in normal and shear stresses of the SWCNTR three layered sandwich composite beam with [90/C/90] under the CC boundary condition. It is observed that there is very small variation in normal and shear stress of core material as compared to face materials due to low elastic modulus.

Table 2 shows the variation of core and laminate thickness on TCD of SWCNTRCSB with load parameter. In this study, five-layer sandwich beam is utilized with [90/30/C/30/90] under CC boundary condition for $a/h=15$, $V_{cnt}=0.25$ and maintaining overall height of sandwich beam is constant ($h=0.35$). As thickness of facesheet and bottom sheet increases simultaneously, the corresponding TCD is reduced down, due to increase in stiffness of face and bottom sheet of SWCNTRCSB. As load increases from 50 to 500, the variation in TCD takes place and observation shows that about 85-87% increment occurs in the TCD in all mentioned thickness combination.

Table 3 shows the three different cases to study the effect of the variation in load parameter, lamina-

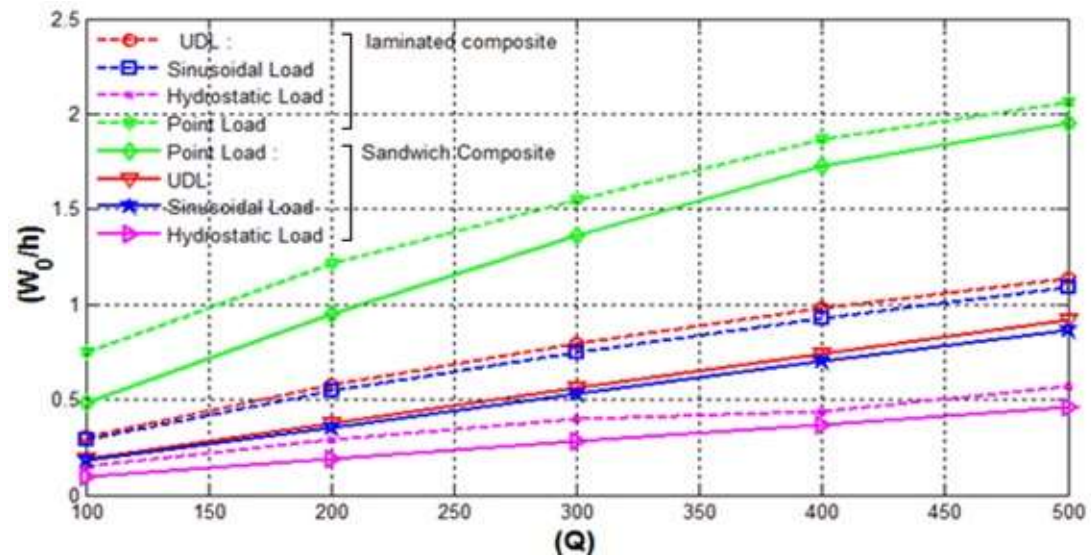


Figure 11

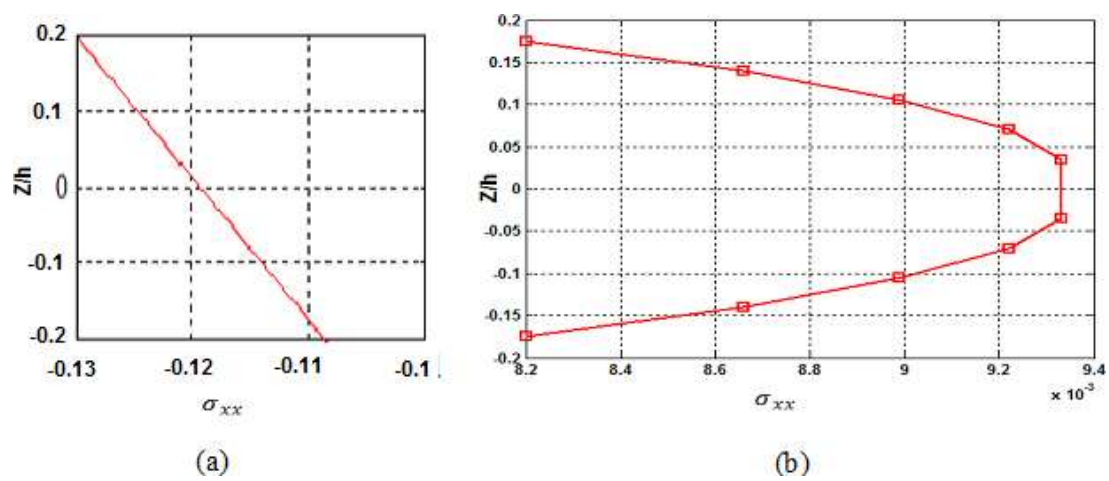


Figure 12

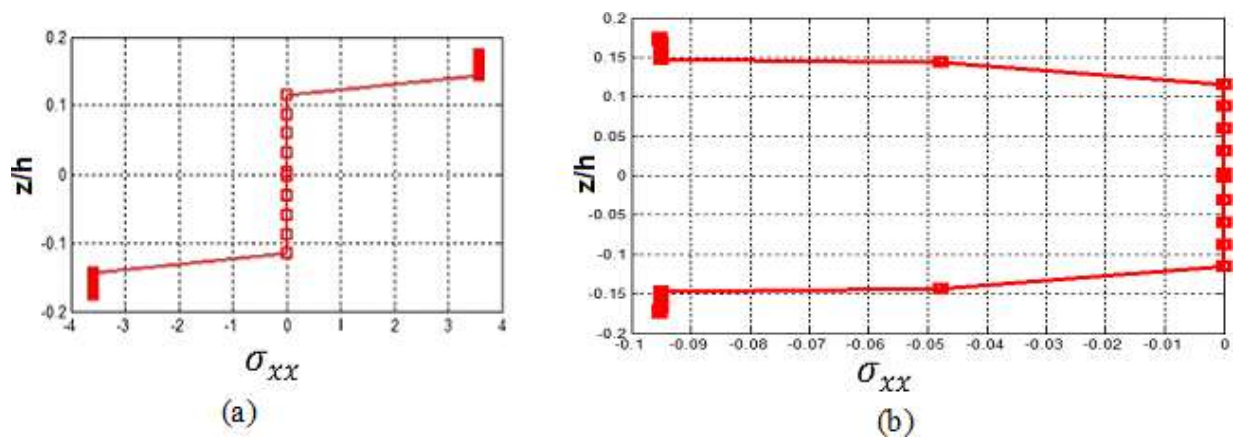


Figure 13

Table 2: Effect of core and sheet thickness variation on transverse central deflection of SWCNTRC sandwich beam

Thickness	α	W_o/h					
		50	100	200	300	400	500
$h_f=0.0175$		0.1867	0.3631	0.6663	0.9077	1.1041	1.269
$h_c=0.28$							
$h_f=0.0194$		0.1597	0.3131	0.5868	0.8140	1.0029	1.164
$h_c=0.2724$							
$h_f=0.0289$		0.0855	0.1702	0.3343	0.4879	0.6291	0.758
$h_c=0.2329$							
$h_f=0.0292$		0.0781	0.1557	0.3073	0.4517	0.5869	0.713
$h_c=0.2332$							
$h_f=0.0375$		0.0618	0.1234	0.2445	0.3616	0.4733	0.579
$h_c=0.200$							

Table 3: Effect of variation in lamination scheme, load parameter and thickness of sandwich beam on transverse central deflection of SWCNTRC sandwich beam

Lamination scheme	α	W_o/h				
		100	200	300	400	500
CASE I						
[90/30/C/30/90]		0.2936	0.5274	0.7072	0.8513	0.9720
[90/30/0/C/90]		0.2505	0.4648	0.6392	0.7825	0.9038
[90/C/0/30/90]		0.2358	0.4421	0.6132	0.7556	0.8768
[90/C/0/C/90]		0.1767	0.3454	0.5009	0.6422	0.7699
[90/C/30/C/90]		0.1767	0.3454	0.5010	0.6423	0.7700
[90/30/0/30/90]		0.5314	0.7999	0.9797	1.1177	1.231
CASE II						
[90/C/90]		0.6170	1.0355	1.3335	1.5656	1.7582
[0/C/0]		0.6144	1.0326	1.3306	1.5629	1.7557
[90/0/90]		1.8792	2.5495	3.0133	3.3716	3.6712
[0/0/0]		1.8744	2.5468	3.0022	3.3610	3.6617
*hf=0.1167						
[0/0/0]		0.2531	0.4822	0.6791	0.8467	0.9912
CASE III						
[90/0/90]		0.3286	0.6105	0.8396	1.0280	1.1862
[0/90/0]		0.3255	0.6056	0.8341	1.0223	1.1805

tion scheme and thickness of the beam namely Case 1 ($h_c=0.15196$; $h_f=0.012$; h_f without core=0.02275), Case 2 ($h_c=0.28$; $h_f=0.035$; h_f without core=0.035), Case 3 ($h_c=0.263$; $h_f=0.0875$) with $V_{cnt}=0.25$, $a/h=0.15$, $T=300K$ under CC support condition for the bending analysis. In Case 1, it is observed that, if core position changes apart from the center, then about 12-14% reduction in the TCD takes place. This is due to load coming from top layer over the core is distributed earlier over entire layer. Further comparison is performed between five layered SWCNTRCB and SWCNTSCB. During the analysis, thickness of individual skin/facesheet and laminate ply thickness is maintained

constant as given in table. It is observed that, as compared to laminated SWCNTRCB very less TCD observed in case of SWCNTSCB, and this shows the major advantage and difference of sandwich laminated composite over the simple laminated composite beam. In Case 2, three layered sandwich and laminated composite beam is considered, and thickness of facesheet/skin is maintained constant in case laminated composite beam also, for the defined lamination scheme. Study shows that about 65% less deflection is observed in case of sandwich composite beam as compared to laminated composite beam. Also if thickness of individual ply increases in case of laminated compos-

Table 4: Effect of various lamination scheme on transverse central deflection of SWCNTRC sandwich beam

Number of walls of CNT	Thickness Ratio	\varnothing	Wo/h				
			100	200	300	400	500
Nw=1	a/h=10		0.31622	0.53895	0.69942	0.82496	0.92875
	a/h=20		0.27815	0.51485	0.70652	0.86351	0.99641
Nw=2	a/h=10		0.36647	0.60217	0.76684	0.89453	0.99985
	a/h=20		0.33126	0.59552	0.79880	0.96191	1.09820
Nw=5	a/h=10		0.38815	0.63476	0.80609	0.93799	1.04681
	a/h=20		0.39277	0.68000	0.89059	1.05710	1.19532

Table 5: Effect of Uniform, linear and nonlinear temperature distribution on transverse central deflection of SWCNT sandwich beam

Loading	T ₁ (K)	T ₂ (K)	Thickness ratio	W _o /h	
				Linear	Non-linear
Uniformly distributed temperature	300	300	5	0.1635	0.2402
	300	300	15	0.2699	0.3878
	350	350	5	0.1623	0.2383
	350	350	15	0.3186	0.479
	400	400	5	0.1611	0.2363
	400	400	15	0.3854	0.7452
Linearly varying temperature	300	350	5	0.1628	0.2392
	300	350	15	0.2849	0.4165
	300	400	5	0.1623	0.2382
	300	400	15	0.3045	0.4559
	300	450	5	0.1617	0.2374
	300	450	15	0.3259	0.5113
	0	300	15	0.0144	0.021
Non-linear varying temperature	300	350	5	0.1631	0.2396
	300	350	15	0.291	0.4224
	300	400	5	0.1627	0.2389
	300	400	15	0.3133	0.4641
	0	0	5	0.1694	0.2498
	0	0	15	0.1306	0.1904
	0	300	5	0.1672	0.2463
	300	0	5	0.1664	0.2450

ite beam by 70%, then there is a drastic reduction in TCD is observed, because of the overall increment in the thickness and so stiffness of laminated composite beam. In Case 3, simple laminated composite beam is studied with 60% more individual ply thickness as compared to three layered sandwich composite beam from case 2. As thickness of ply/ laminate increases then there is less TCD produced in the beam. From the Table 3, it is concluded that, for the same individual ply thickness of facesheet, bottom sheet and laminate, drastic difference in TCD is observed which is minimum in case of sandwich beam. That shows the performance superiority of sandwich composite over laminated composite beam.

In Table 4, the effect of MWCNT and thickness ratio is observed over TCD under CC boundary condition, 300K, V_{cnt}=0.25 and [90/30/C/30/90]. It is clearly observed from the table that, whenever shifting from SWCNT to MWCNT, with variation in thickness ratio, TCD of SWCNTSCB increases, because transverse resistance of SWCNT is more than MWCNT, and this is due to elastic moduli is more in case of SWCNT.

Table 5 elaborate the variation in the TCD with uniform, linear and non-linear varying temperature distribution in the SWCNTSCB with load of 100, V_{cnt}=0.2, a/h=15, [0/C/0] and CC boundary condition. From the table, it is clear that, as temperature increases, it directly affect

on the TCD of sandwich beam. In case of uniformly distributed temperature, average change in sandwich beam deflection is 16-20%, but it is 38-40% if thickness ratio is decreased. In case of linearly varying temperature it is 10% while, in non-linear varying temperature distribution it is 10-12%. So there is a maximum TCD deflection occurs in case of uniformly distributed temperature variation. So need to give attention whenever the body or specimen is under uniform temperature distribution. Also whenever the linear temperature variation is from 0 to 300K, then the deflection due to linear temperature distribution is small as compared to non-uniform temperature distribution because of uniformity in variation of temperature.

4 Conclusions

In this paper, three and five layered SWCNTRC and MWCNTRC sandwich composite beam is studied under thermal and mechanical loading using HSDT and Von Kármán non-linearity through FEM using MATLAB subroutine. Study gives the following observations,

Among the different boundary conditions, minimum transverse central deflection for laminated sandwich composite beam is observed at CC supported condition due to more number of constraints in provided boundary condition. As compared to CF, about 50% less deflection is observed in case of CC support condition.

As the volume fraction of CNT increases, the transversal deflection in the beam reduced down and maximum transverse deflection is observed at the center of the beam. it is also observed that, for 0.1% CNT volume fraction, there is approximately 51-52% decrease in deflection, for 0.2% CNT volume fraction, there is approximately 47-48% decrease in deflection, for 0.3% CNT volume fraction, there is approximately 46-47% decrease in deflection and for 0.4% CNT volume fraction, there is approximately 45-46% decrease in deflection.

As thickness ratio (a/h) increases, the transvers deflection of the beam also increases and this is due to decrease in the transverse resistant with respect to beam thickness.

There is a minimum TCD produced in sandwich composite beam as compared to SWCNTR laminated composite beam, also the point loading shows the highest deflection as compared to other loadings due to application over the point or minimum area. Also TCD produced in case of UDL is 5-7% and about 50% more as compared to sinusoidal and hydrostatic load respectively for the sandwich and laminated composite beam.

If core position changes apart from the center, then about 12-14% reduction in the TCD takes place. This is due to load coming from top layer over the core is distributed earlier over entire layer. Further comparison is performed between five layered SWCNTRCB and SWCNTSCB, as compared to laminated SWCNTRCB very less TCD observed in case of SWCNTRSCB, and this shows the major advantage and difference of sandwich laminated composite over the simple laminated composite beam

In case of SWCNTR three layered laminated composite beam the effect of longitudinal stress is higher as compared to transverse stress, also very small variation in normal and shear stress of core material as compared to face materials due to low elastic modulus in case of SWCNTR three layered sandwich composite beam.

References

- [1] Shen H.S., Nonlinear bending of functionally graded carbon nanotube-reinforced composite plates in thermal environments, *Compos. Struct.*, 2009, 91, 9-19.
- [2] Fidelus J.D., Wiesel E., Gojny F.H., Schulte K., Wagner H.D., Thermo-mechanical properties of randomly oriented carbon/epoxy nanocomposite, *Compos. Part A*, 2005, 36, 1555-1561.
- [3] Anumandla V., Gibson R.F., A comprehensive closed form micromechanics model for estimating the elastic modulus of nanotube-reinforced composites, *Compos. Part A*, 2006, 37, 2178-2185.
- [4] Shen H.S., Xiang Y., Nonlinear analysis of nanotube reinforced composite beams resting on elastic foundations in thermal environments, *Engg. struct.*, 2013, 56, 698-708.
- [5] Ghafaar M.A., Mazen A.A., El-Mahallawy N.A., Application of the rule of mixtures and Halpin-Tsai equations to woven fabric reinforced epoxy composites, *Journal of Engineering Sciences*, 2006, 34(1), 227-236.
- [6] Kundalwal S.I., Review on Micromechanics of Nano- and Micro-Fiber Reinforced Composites, *Poly. Compos.*, 2017, 39-12. DOI 10.1002/pc.24569
- [7] Banerjee S., Sankar B.V., Mechanical properties of hybrid composites using finite element method based micromechanics, *Compos. Part B: Engg.*, 2014, 58, 318-327.
- [8] Kim H.G., Lee K.K., Evaluation of elastic modulus for unidirectionally aligned short fiber composites, *Journal of Mech. Sci. and Tech.*, 2009, 23, 54-63.
- [9] Kim M., Mirza F.A., Song J.I., Micromechanics modeling for the stiffness and strength properties of glass fibers/CNTs/epoxy composites, *High Performance Structures and Materials V*, WIT Transactions on the Built Environment, 112, WIT Press, 2010.
- [10] Kormaníková E., Kotrasová K., Elastic Mechanical Properties of Fiber Reinforced Composite Materials, *Chem. Listy.*, 2011, 105, 758-762.
- [11] Lal A., Markad K.M., Thermo-Mechanical Post Buckling Analysis of Multiwall Carbon Nanotube-Reinforced Composite Laminated Beam under Elastic Foundation, *Curved and Layer Struct.*, 2019,

- 6, 212-228.
- [12] Liu L., Huang Z., A Note on Mori-Tanaka's method, *Acta Mechanica solida sinica*, 2014, 27(3).
 - [13] Alebrahim R., Sharifishourab G., Sharifi S., Alebrahim M., Zhang H., Yahya Y., Ayob A., Thermo-mechanical behaviour of smart composite beam under quasi-static loading, *Compos. Struct.*, 2018, 201, 21-28.
 - [14] Xiong J., Vaziri A., Li Ma, Jim P., Wu L., Compression and impact testing of two layer composite pyramidal-core sandwich panels, *Compos. Struct.*, 2011, 94(2), 793-801. doi:10.1016/j.compstruct.2011.09.018
 - [15] Wang B., Wu L. Z., Li Ma, Feng J.C., Low-velocity impact characteristics and residual tensile strength of carbon fiber composite lattice core sandwich structures, *Compos. Part B*, 2011, 42, 891-897.
 - [16] Wang S.X., Wu L.Z., Li Ma, Low-velocity impact and residual tensile strength analysis to carbon fiber composite laminates. *Mat. and Design*, 2010, 31(1), 118-125.
 - [17] Mantari J.L., Oktem A.S., Soares C.G., A new trigonometric shear deformation theory for isotropic, laminated composite and sandwich plates, *Inter. journal of solids and struct.*, 2012, 49, 43-53.
 - [18] Sahoo R., Singh B.N., A new shear deformation theory for the static analysis of laminated composite and sandwich plates, *Inter. Journal of Mech. Sci.*, 2013, 75, 324-336.
 - [19] Zhao R., Yu K., Hulbert G.M., Wu Y., Li X., Piecewise shear deformation theory and finite element formulation for vibration analysis of laminated composite and sandwich plates in thermal environments, *Compos. Struct.*, 2017, 160, 1060-1083.
 - [20] Mantari J.L., Soares C.G., Generalized layerwise HSDT and finite element formulation for symmetric laminated and sandwich composite plates, *Compos. Struct.*, 2013, 105, 319-331.
 - [21] Vidal P., Gallimard L., Polit O., Thermo-mechanical analysis of laminated composite and sandwich beams based on a variables separation, *Composite Structures*, 2016, 152, 755-766.
 - [22] Li Z.Q., Song H.P., Tang H.P., Wang Z.H., Zhao L.M., Thermal-mechanical behavior of sandwich panels with closed-cell foam core under intensive laser irradiation, *Therm. Sci.*, 2014, 18(5), 1607-1611.
 - [23] Santiuste C., Thomsen O.T., Frostig Y., Thermo-mechanical load interactions in foam cored axi-symmetric sandwich circular plates - High-order and FE models, *Compos. Struct.*, 2011, 93(2), 369-376.
 - [24] Lal A., Markad K.M., Deflection and stress behaviour of multi-walled carbon nanotube reinforced laminated composite beams, *Computers and concrete*, 2018, 22(6), 501-514.
 - [25] Karamanli A., Bending analysis of composite and sandwich beams using Ritz method, *Anadolu uni. Jou. of sci. and tech. A- Applied sciences and engg.*, 2018, 19, 10-23.
 - [26] Ghugal Y.M., Shikhare G.U., Bending analysis of sandwich beams according to refined trigonometric beam theory, *Journal of Aerospace Engineering & Technology*, 2015, 5(3), 27-37.
 - [27] Gibson R.F., A simplified analysis of deflections in shear deformable composite sandwich beams, *Journal of Sandwich Struct. and Mat.*, 2011, 13(5), 579-588.
 - [28] Yoon K.J., Kim C.K., Park H.C., Nonlinear flexural deflection of thermoplastic foam core sandwich beam, *Journal of compos. Mat.*, 2002, 36(13), 1529-1539.
 - [29] Thorat S.R., Rathi V.R., Sayyad A.S., Bending analysis of sandwich beam with soft core, *International research journal of engineering and technology*, 2018, 5(5), 2780-2784.
 - [30] Sayyada A.S., Ghugal Y.M., Static flexure of soft-core sandwich beams using trigonometric shear deformation theory, *Mecha.of advanced compos. Struct.*, 2015, 2, 45-53.
 - [31] Li H., Zhu X., Mei Z., Qiu J., Zhang Y., Bending of orthotropic sandwich plates with a functionally graded core subjected to distributed loadings, *Acta Mecha. Solida Sinica*, 2013, 26(3), 292-301.
 - [32] Bhardwaj G., Upadhyay A.K., Pandey R., Shukla K.K., Non-linear flexural and dynamic response of CNT reinforced laminated composite plates, *Compos. Part B*, 2013, 45, 89-100.
 - [33] Kumar P., Srinivas J., Free Vibration, bending and buckling behavior of FG-CNT reinforced composite beam: comparative analysis with hybrid laminated composite beam, *Multidiscipline modeling in mat. and struct.*, 2017, 13(4), 590-611.
 - [34] Deng J., Lee M.M.K., Behaviour under static loading of metallic beams reinforced with a bonded CFRP plate, *Compos. Struct.*, 2007, 78(2), 232-242.
 - [35] Rouhi S., Alavi S.H., On the mechanical properties of functionally graded materials reinforced by carbon nanotubes, *Proceedings of the Institution of Mechanical Engineers, Part C: Journal of Mech. Engg. Sci.*, 2017, 232(9), 1632-1646.
 - [36] Singh B.N., Lal A., Kumar R., Nonlinear bending response of laminated composite plates on nonlinear elastic foundation with uncertain system properties, *Engg. Struct.*, 2008, 30, 1101-1112.
 - [37] Shen H.S., Feng L., Xiang Y., Nonlinear bending and thermal post-buckling of functionally graded graphene-reinforced composite laminated beams resting on elastic foundations, *Engg. Struct.*, 2017, 140, 89-97.
 - [38] Ferreira A.J.M., MATLAB codes for finite element analysis, Springer, ISBN: 978-1-4020-9199-5, 2009.
 - [39] Donthireddy P., Chandrashekhara K., Nonlinear Thermomechanical analysis of laminated composite beams, *Advanced Compos. Mat.*, 1997, 6(2), 153-166.
 - [40] Kim N., Lee J., Geometrically nonlinear coupled analysis of thin-walled Al/Al₂O₃ FG sandwich box beams with single and double cells, *Acta Mech*, 2018, 229, 4677-4699.
 - [41] Gdoutos E.E., Zacharopoulos D.A., Aluminum/Foam Sandwich Beams in Three-Point Bending, In: Gdoutos E.E. (eds) *Experimental Analysis of Nano and Engineering Materials and Structures*, 2007, Springer, Dordrecht.